Structural, electronic and optical properties of semiconducting rhenium silicide

2004 J. Phys.: Condens. Matter 16 303

(http://iopscience.iop.org/0953-8984/16/3/010)

INSTITUTE OF PHYSICS PUBLISHING JOURNAL OF PHYSICS: CONDENSED MATTER

J. Phys.: Condens. Matter **16** (2004) 303–312 PII: S0953-8984(04)70286-6

Structural, electronic and optical properties of semiconducting rhenium silicide

V L Shaposhnikov[1,5], A V Krivosheeva[1], L I Ivanenko[1], A B Filonov[1], V E Borisenko[1], M Rebien[2], W Henrion[2], D B Migas[3], L Miglio[3], G Behr[4] and J Schumann[4]

[1] Belarusian State University of Informatics and Radioelectronics, P Browka 6, 220013 Minsk, Belarus
[2] Hahn–Meitner Institute, Kekuléstraße 5, D-12489 Berlin, Germany
[3] INFM and Dipartimento di Scienza dei Materiali, Universita di Milano-Bicocca, via Cozzi 53, 20125 Milano, Italy
[4] Leibniz Institute of Solid State and Materials Research, POB 27 01 16, D 01171 Dresden, Germany

E-mail: victor@fis.ua.pt (V L Shaposhnikov)

Received 11 October 2003
Published 9 January 2004
Online at stacks.iop.org/JPhysCM/16/303 (DOI: 10.1088/0953-8984/16/3/010)

Abstract

Structural, electronic and optical properties of semiconducting rhenium silicide ($ReSi_{1.75}$) with various distributions of the silicon vacancies have been theoretically studied by means of ultrasoft pseudopotential and full-potential linearized augmented plane wave methods. We have found that the band dispersion is affected by vacancy positions, while the dielectric function and reflectivity display similar shapes for all considered variants, that can explain the rather scattered available experimental data on the gap value. Comparison between the calculated and ellipsometrically measured dielectric function and reflectivity on $ReSi_{1.8}$ polycrystals grown by the Czochralski technique shows a good agreement.

(Some figures in this article are in colour only in the electronic version)

1. Introduction

Semiconducting transition-metal silicides have been given considerable attention due to their possible applications in microelectronic device technology [1]. Among them rhenium silicide ($ReSi_{1.75}$), being a narrow-gap semiconductor, was used for fabrication of infrared-sensing devices [2]. In order to achieve maximum efficiency of such devices the fundamental properties of the silicide, which are known to be contradictory, must be investigated in detail. In fact, experimentally reported values of the bandgap vary from 0.11 to 0.36 eV [3–9]. Absorption

[5] Present address: Department of Physics, University of Aveiro, 3810-193 Aveiro, Portugal.

measurements performed on thin films show an indirect gap of 0.15 eV [3, 4], whereas optical transmittance and reflectance indicate the indirect and direct gaps to be 0.12 and 0.36 eV, respectively [5]. An energy gap of 0.21 eV was estimated by reflectivity and resistivity measurements [6]. Resistivity and transport experiments on a single crystal demonstrate two gaps of 0.16 and 0.30 eV [7] while the bandgap of 0.28 eV is obtained on thin films [8] and sizable variations in the gap value (0.11–0.36 eV) are reported to be closely connected with preparation conditions of thin films.

Rather scattered data can also be found on the crystal structure of rhenium silicide: tetragonal ($ReSi_2$ [6] and $ReSi_{1.8}$ [10] stoichiometry) and triclinic [7, 11] or monoclinic [9] ($ReSi_{1.75}$ stoichiometry). The $ReSi_{1.75}$ stoichiometry, in which some of the Si sites are partially occupied, is shown to be important in order to provide semiconducting properties [12]. The first-principles calculations by means of the linear muffin-tin (LMTO) method [12] and the linearized augmented plane wave (LAPW) method [13] have been performed without relaxation of the crystal structure, displaying respectively an indirect gap of 0.16 eV and the gapless nature of $ReSi_{1.75}$. The optical functions and the influence of a random distribution of the Si vacancies in the crystal on silicide properties have never been addressed before.

In this paper we present *ab initio* total-energy estimates, band structures, dielectric function and reflectivity of $ReSi_{1.75}$ with various configurations of the Si vacancies in the unit cell. We apply the ultrasoft pseudopotential (USPP) method, perfectly suitable for the total-energy calculations and the full structural optimisation, as well as the full-potential linearized augmented plane wave (FLAPW) method for the calculation of the band structure and optical functions using lattice parameters and atomic positions of the silicide fully optimized by USPP. The results of original ellipsometric and reflectivity measurements on $ReSi_{1.8}$ polycrystals in comparison with theoretical data are also reported.

2. Experiment

2.1. Sample preparation and characterization

Polycrystalline $ReSi_{1.8}$ was prepared from 4 N Re powder (Goodfellow) and 6 N Si (Alfa). The starting materials were melted together in an arc melting facility under purified argon atmosphere. The growth process without a seed crystal was performed by the Czochralski technique from a Hukin-type cold crucible. The pulling rate was 2.8 μm s^{-1} and the rotation 0.33 s^{-1}. The crystal grown was 30 mm in length and 12 mm in diameter and showed single-crystalline grains more than 10 mm long and about 2 mm in the cross section. Some cracks were observed inside. The composition, microstructure and perfection of the crystals were investigated by x-ray diffraction analysis, optical metallography and electron probe microanalysis applying the energy dispersive mode. The samples were single phase with an orthorhombic structure and lattice parameters $a = 3.122$ Å, $b = 3.137$ Å and $c = 7.670$ Å. The composition of the samples, measured by electron microprobe in the energy dispersive mode, was close to $ReSi_{1.8}$. From the crystal, slices about 10 mm in diameter and 1 mm thick were cut by a diamond saw.

2.2. Experimental details

Room temperature reflection spectra from 0.5 to 6.2 eV were measured using a commercial spectrophotometer. The specularly and diffusely reflected light was recorded by an integrating sphere. Due to the high absorption of the samples no transmission spectra could be measured. Spectroscopic ellipsometry measurements at room temperature were carried out

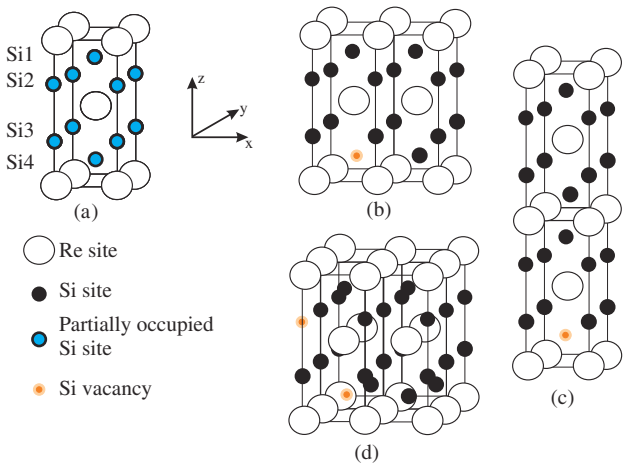

Figure 1. Structural models of crystal structure of $ReSi_{1.75}$. (a) Unit cell; (b) the $2a\ b\ c$ configuration; (c) the $a\ b\ 2c$ configuration; (d) the $2a\ 2b\ c$ configuration.

on a Woollam Co. VASE ellipsometer over the photon energy range 0.75–4.5 eV at an angle of incidence of $75.00° \pm 0.02°$. In order to extract the bulk dielectric function values from the extremely surface sensitive ellipsometric spectra, a model has to be established taking into account the native oxide overlayer, microscopic surface roughness and small voids present on the polished sample surface.

A native oxide layer consisting mainly of SiO_2 is commonly observed on silicon-rich metal silicide surfaces [14]. As the exact measurement of oxide thickness and refractive index in this range is extremely difficult, a thickness value of 2 nm SiO_2 was estimated. SiO_2 optical constants were taken from tabulated data [15].

The good agreement between the reflectivity values measured directly at near-normal incidence and the near-normal incidence reflectivity spectrum calculated from the ellipsometric data determined at a large angle of incidence confirms the modelling procedure of the ellipsometric measurements.

3. Details of calculations

3.1. Structural models

Both x-ray diffraction and transmission electron microscopy investigations on single crystals [7] and alloys [11] of $ReSi_{2-x}$ show this silicide to possess the off-stoichiometric composition $ReSi_{1.75}$. Its crystal structure is found to be triclinic (space group $P1$, $a = 3.138$ Å, $b = 3.120$ Å, $c = 7.67$ Å and $\alpha = 89.9°$; for details see [7]) due to slight distortion from the tetragonal ($C11b$ type) structure where some silicon sites have a partial occupancy (see figure 1(a)). Misra *et al* [11] reported just one such site (occupancy factor 0.5) whereas Gottlieb *et al* [7] indicated two sites (occupancy factor 0.75).

In order to take into account an integer number of each type of atom, the unit cell (depicted in figure 1(a)) should be enlarged twice along one or two axes, respectively. In this work we study the following variants: $2a\ b\ c$, $a\ b\ 2c$ and $2a\ 2b\ c$, which are shown in figures 1(b)–(d), respectively. Note that the $2a\ b\ c$ and $a\ 2b\ c$ configurations are equal and any of the silicon sites can be vacant because of the tetragonal origin of the triclinic structure. In the case of

$2a\ 2b\ c$ we also considered different possible positions of silicon vacancies in the enlarged unit cell, namely Si3 and Si4, Si2 and Si3, and Si2 and Si4, which are equivalent to Si1 and Si2, Si1 and Si4, and Si1 and Si3, respectively.

3.2. Methods

Total-energy calculations and full structural optimization have been performed by the *ab initio* code VASP (Vienna *ab initio* Simulation Package) with plane-wave basis-set and ultrasoft pseudopotentials. This code has been described in detail elsewhere [16]. In our study we used the local density approximation (LDA) of Ceperly and Alder with the parametrization of Perdew and Zunger [17]. Ultrasoft Vanderbilt-type pseudopotentials have been employed for the $5d^6 6s^1$ and $3s^2 3p^2$ atomic configurations of Re and Si, respectively. Nonlocal contributions were evaluated using the reciprocal projection scheme. Total-energy minimization, via lattice parameter optimization and atomic position relaxation in a conjugate gradient routine, was obtained by calculating the Hellmann–Feynman forces and the stress tensor including the Pulay correction to compensate for changes in the basis set due to variation in the shape of the unit cell. We found that the convergence in the total energy was better than 1 meV/atom using the energy cut-off of 400 eV and the $4 \times 8 \times 4$, $8 \times 8 \times 4$ and $4 \times 4 \times 4$ grids of Monkhorst–Pack points for the $2a\ b\ c$, $a\ b\ 2c$ and $2a\ 2b\ c$ configurations, respectively. The bulk modulus was calculated by fitting the total energies at different unit-cell volumes on a Murnaghan equation of state.

The electronic and optical properties of rhenium silicide have been calculated by the self-consistent FLAPW method (WIEN2K package [18]). We use the LDA of Ceperly and Alder with the parametrization of Perdew and Zunger [17] as well as structural parameters fully optimized by USPP. Within the muffin-tin spheres, lattice harmonics with angular momentum l up to ten are used to expand the charge density, the potential and the wavefunctions. The muffin-tin radii R_{MT} have been set to 2.2 au for both metal and silicon atoms. The calculations were performed with the energy cut-off constant $R_{\mathrm{MT}} K_{\max} = 8$. Self-consistent procedures were done on a grid of 51 **k**-points uniformly distributed in the irreducible part of the Brillouin zone. Further increase of the cut-off and **k**-point numbers did not exert an essential influence on the eigenvalues. The band structure has been plotted with 20 **k**-points for each segment along the high-symmetry directions. The dipole matrix elements were computed in the onsite-transition approximation on a dense mesh of 545 **k**-points. The interband contribution to the imaginary part of the dielectric function (ε_2) was calculated within the random-phase approximation, neglecting local-field and finite-lifetime effects, as

$$\varepsilon_2^{\alpha}(\omega) = \frac{4\pi^2 e^2}{m^2 \omega^2 V_{\mathrm{BZ}}} \sum_{v,c,\mathbf{k}} |\langle \psi_{c\mathbf{k}} | p_{\alpha} | \psi_{v\mathbf{k}} \rangle|^2 \cdot \delta(E_{c\mathbf{k}} - E_{v\mathbf{k}} - \hbar\omega), \tag{1}$$

where p_{α} is the projection of the momentum matrix element along the α-direction of the electric field ($\alpha = x, y, z$), $E_{c\mathbf{k}}$ and $E_{v\mathbf{k}}$ are the one-electron energies of the valence $\psi_{v\mathbf{k}}$ and conduction $\psi_{c\mathbf{k}}$ band states at the **k**-point and V_{BZ} is the Brillouin zone volume. To obtain the corresponding real part (ε_1) of the dielectric function the Kramers–Kronig relation was applied.

4. Results and discussion

4.1. Structural properties of $ReSi_{1.75}$

In spite of the big similarity in the lattice constants and angles for the $2a\ 2b\ c$, $2a\ b\ c$ and the $a\ b\ 2c$ configurations (see table 1) the latter is found to be sizably higher in energy

Table 1. Optimized lattice constants a, b and c (Å) and angles α, β and γ, cohesive energies E_{coh} (eV/atom) and bulk modulus B_0 (Mbar) for the various configurations of $ReSi_{1.75}$ and tetragonal $ReSi_2$ in comparison with the experimental data.

	$ReSi_2$	2*a b c*	*a b* 2*c*	2*a* 2*b c* Si3 and Si4	2*a* 2*b c* Si2 and Si3	2*a* 2*b c* Si2 and Si4	Experiment [this work]	Experiment [7]
a	3.147	3.090	3.117	3.094	3.086	3.086	3.122	3.138
b	3.147	3.095	3.117	3.094	3.080	3.085	3.137	3.120
c	7.758	7.672	7.688	7.696	7.683	7.678	7.670	7.670
α (deg.)		∼90[a]	89.8	89.8	∼90[a]	∼90[a]		89.9
β (deg.)		∼90[a]	89.8	89.8	∼90[a]	∼90[a]		90
γ (deg.)		∼90[a]	∼90[a]	89.8	∼90[a]	∼90[a]		90
E_{coh}		9.232	9.136	9.227	9.230	9.231		
B_0	2.47	2.52	2.43	2.51	2.54	2.54		1.65[b]

[a] ∼90° indicates that the deviation from 90° is less than 0.05°.
[b] Reference [21].

by ∼0.1 eV/atom, indicating that the enlargement of the unit cell along the *c*-axis is not favourable, and we excluded this case from further consideration. The energy difference between the other variants is marginal (∼0.005 eV/atom) and their lattice parameters, being very close to the experimental ones, are smaller than those of tetragonal $ReSi_2$. The evaluated bulk modulus of $ReSi_{1.75}$ is comparable with values for other transition-metal silicides [19, 20], but still displays a little discrepancy with experimental data [21]. It is quite probable that the experimental result can be affected by a crystal imperfection, whereas theoretical estimates with generalized gradient corrections to LDA usually provide a smaller value of the bulk modulus which would be closer to the experimental one. For simplicity reasons in band structure and optical property calculations we treat $ReSi_{1.75}$ as having a simple orthorhombic structure due to the slight deviation of the α, β and γ angles from 90°.

4.2. Band structure

The band structures of the 2*a* 2*b c* and 2*a b c* variants are found to be gapless independently of USPP and FLAPW calculations and we rigidly shifted the conduction band up (approximately by 0.4–0.55 eV). In figure 2 we report the corresponding band diagrams displaying the gap value of 0.16 eV in order to reproduce the experimentally observed size and the result obtained by the LMTO method [12]. It is clearly seen that the shape of the bands close to the gap for the 2*a* 2*b c* configuration with silicon vacancies in Si3 and Si4 or Si2 and Si4 (see figures 2(b) and (d), respectively) is similar to that presented in [12], where the former variant has been taken into account. Moreover, for all cases considered, the dispersion of the last valence band is close: very flat along the Γ–Z direction due to the pure Re-d character [12] and the presence of a second maximum at the S point is evident (only for the 2*a* 2*b c* variants). Note also that for the 2*a* 2*b c* variants the corresponding Brillouin zone is folded along the *y*-direction with respect to that of the 2*a b c* variant. In contrast to the top of the valence band the dispersion of the first conduction band is found to be different for the 2*a* 2*b c* configurations, in particular when two Si vacancies (Si2 and Si3) are aligned along the *z*-direction (compare figures 2(c) and (b), (d)). In fact, the minimum of the conduction band is at the 0.7 × Γ–X point (figure 2(c)) or at the S point (figures 2(b) and (d)) and in the former case the sizable lowering of the first conduction band along the Γ–Z–U directions is clearly seen.

The bandgap energies calculated by density functional methods are usually underestimated with respect to experimental ones, while an anomalous discrepancy with respect to the LMTO

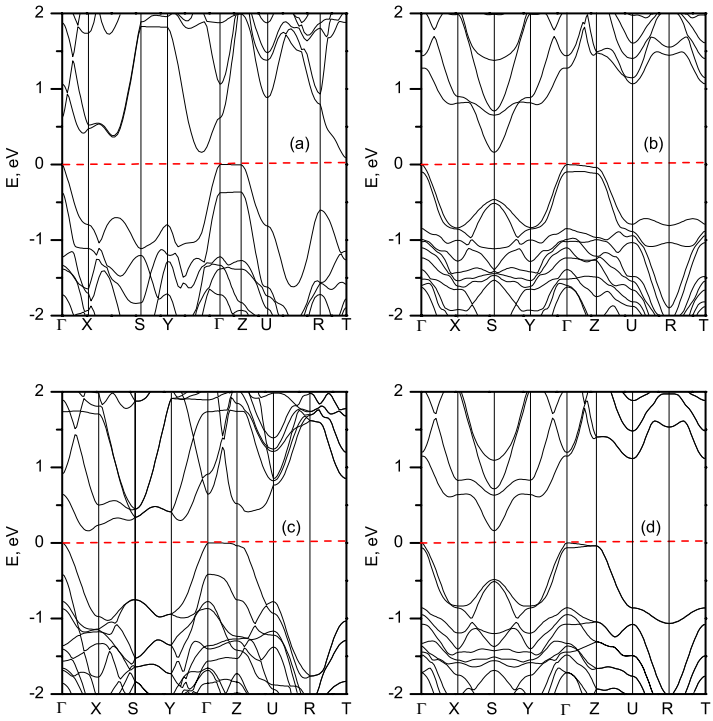

Figure 2. Band structure of $ReSi_{1.75}$ with different positions of the Si vacancies in the unit cell: (a) the 2*a b c* configuration; (b) the 2*a* 2*b c* configuration with Si vacancies in Si3 and Si4; (c) the 2*a* 2*b c* configuration with Si vacancies in Si2 and Si3; (d) the 2*a* 2*b c* configuration with Si vacancies in Si2 and Si4. Zero on the energy scale corresponds to the Fermi energy.

result [12] is evident. However, our LMTO predictions on bandgap energies for other transition-metal silicides provide larger values than those obtained by FLAPW and USPP. For example, the gaps of 0.02 and −0.03 eV were estimated by FLAPW [22] for hexagonal $MoSi_2$ and WSi_2, respectively, to be compared to 0.07 eV of LMTO [23], and in the case of β-$FeSi_2$ the difference is found to be about 0.1 eV (see [24–26]). In order to confirm the last issue we have performed an additional calculation by USPP and FLAPW using the experimental lattice parameters and atomic positions, as in the case of [12], and revealing again the gapless character, that is in agreement with the LAPW results [13]. Such a discrepancy in bandgap energies by LMTO and by USPP, FLAPW and LAPW may stem from the fact that the data obtained by LMTO are usually sensitive to a choice of muffin-tin radii as pointed out in [20].

4.3. Dielectric function and reflectivity

The calculated ε_1, ε_2 and R for the $E \parallel c$ and $E \perp c$ light polarizations are shown in figure 3. It should be noted here that the spectra for the *a* and *b* light polarizations coincide because of the tetragonal origin of the $ReSi_{1.75}$ unit cell. We found these optical functions to display the same shape for any variant considered, indicating independence from the Si vacancy positions. It is also evident that ε_1, ε_2 and R are anisotropic in the energy range analysed. In fact, in the case of ε_2 the main maximum for $E \parallel c$ is at 3.6 eV, 1.4 eV lower in energy than that for $E \perp c$. Another feature worth discussing here is the small oscillator strength of low-lying direct transitions. This issue can be confirmed by analysing dipole matrix elements

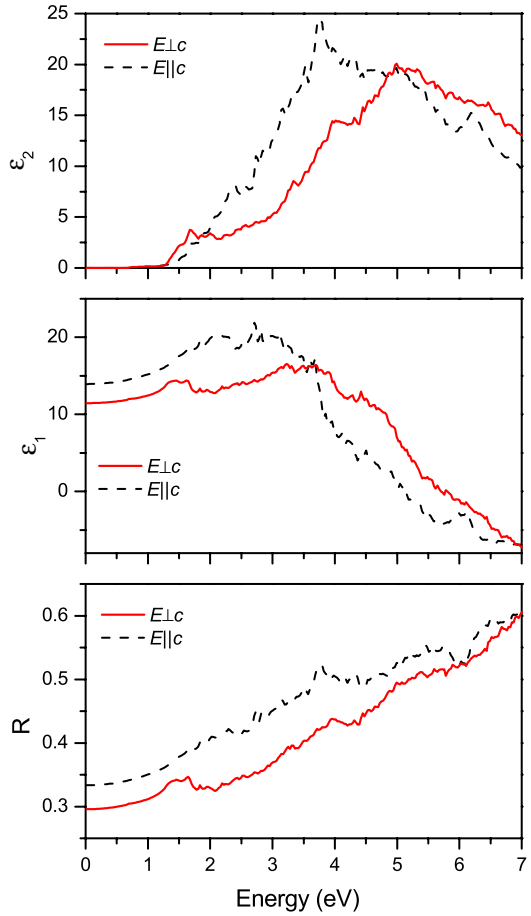

Figure 3. The imaginary (ε_2) and real (ε_1) parts of the dielectric function and the reflectivity (R) of $ReSi_{1.75}$ versus photon energy for different light polarizations as calculated by FLAPW with LDA.

corresponding to transitions at the S-, Γ- and Z-points (the $2a$ $2b$ c configurations) for which numerical estimates resulted in a very small value due to the dominating Re-d character across the gap [12]. Meanwhile, the rapid start of ε_2 at higher energies can be attributed to the joint density of interband states. Such a low value of oscillator strength of the low-lying direct transitions and anisotropy of optical functions are typical of transition-metal silicides [19, 25].

The dependences of the imaginary and real parts of the dielectric function and the reflectivity of $ReSi_{1.8}$ crystals on the photon energy, as obtained by ellipsometric and reflectivity measurements, are presented in figure 4. These spectra are close in shape to those reported in [6] where polycrystaline samples of $ReSi_{1.96}$, prepared by arc melting, were investigated. Thus, the position of the main maximum of ε_2 in our case is at 3.4 eV, to be compared to 3.3 eV [6]. The latter issue points out that the optical spectra are not sensitive to the Si content in the silicide. Since only polycrystalline samples of $ReSi_{1.8}$ have been investigated in our work, an average of computed spectra for the different light polarizations has been used. Comparison between experimental and theoretical ε_1, ε_2 and R shows a good agreement as can be seen in figure 4.

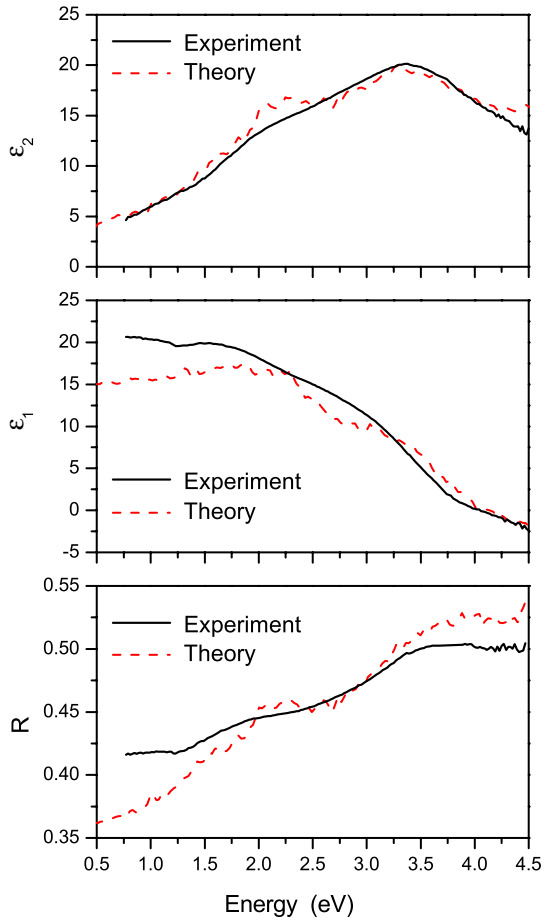

Figure 4. The average of the theoretically calculated imaginary (ε_2) and real (ε_1) parts of the dielectric function and the reflectivity (R) of $ReSi_{1.75}$ versus photon energy compared with experimental data.

5. Conclusions

We have carried out a theoretical study of structural, electronic and optical properties of semiconducting rhenium silicide with various configurations of the silicon vacancies. The performed full optimization of the $ReSi_{1.75}$ crystal structure indicates many possible variants of Si vacancy distribution in the unit cell while displaying negligible differences in energy and similar lattice parameters. Unfortunately, we cannot make predictions on the gap value because of the gapless character. Nevertheless, the different dispersion of the first conduction band for all cases considered is revealed. We believe that this issue may be responsible for rather scattered experimental data on the value of the gap (0.11–0.36 eV) [3–9] and on transport properties observed in (post-deposition) thermal measuring cycles probably caused by silicon vacancy kinetics during high-temperature exposure [27]. However, the calculated optical functions (ε_1, ε_2 and R) are not affected by positions of the Si vacancies, also demonstrating a good agreement with the results of ellipsometric and reflectivity measurements.

References

[1] Borisenko V E (ed) 2000 *Semiconducting Silicides* (Berlin: Springer)

[2] Becker J P, Mahan J E and Long R G 1995 $ReSi_2$ thin-film infrared detectors *J. Vac. Sci. Technol.* A **13** 1133–5

[3] Nguyen Tan T A, Veuillen J Y, Muret P, Kennou S, Siokou A, Ladas S, Lahatra Razafindramisa F and Brunel M 1995 Semiconducting rhenium silicide thin films on Si(111) *J. Appl. Phys.* **77** 2514–8

[4] Ali I, Muret P and Nguyen Tan T A 1996 Properties of semiconducting rhenium silicide thin films grown epitaxially on silicon (111) *Appl. Surf. Sci.* **102** 147–50

[5] Long R G, Bost M C and Mahan J E 1988 Optical and electrical properties of semiconducting rhenium disilicide thin films *Thin Solid Films* **162** 29–40

[6] Siegrist T, Hulliger F and Travaglini G 1983 The crystal structure and some properties of rhenium silicide ($ReSi_2$) *J. Less-Common Met.* **92** 119–29

[7] Gottlieb U, Lambert-Andron B, Nava F, Affronte M, Laborde O, Rouault A and Madar R 1995 Structural and electronic transport properties of $ReSi_{2-\delta}$ single crystals *J. Appl. Phys.* **78** 3902–7

[8] Ali I, Muret P and Haydar A 2001 Electrical transport properties of semiconducting rhenium silicide thin films on silicon (111) *Semicond. Sci. Technol.* **16** 966–71

[9] Kuwabara K, Inui H and Yamaguchi M 2002 Microstructure and electrical properties of thin films of $ReSi_{1.75}$ produced by co-sputtering *Intermetallics* **10** 129–38

[10] Jorda J L, Ishikawa M and Muller J 1982 Phase relations and superconductivity in the binary Re–Si system *J. Less-Common Met.* **85** 27–35

[11] Misra A, Chu F and Mitchell T E 1999 Incommensuration and other structural anomalies in rhenium disilicide *Phil. Mag.* A **79** 1411–22

[12] Filonov A B, Migas D B, Shaposhnikov V L, Dorozhkin N N, Borisenko V E, Lange H and Heinrich A 1999 Electronic properties of semiconducting rhenium silicide *Europhys. Lett.* **46** 376–81

[13] Kurganskii S I, Pereslavtseva N S, Levitskaya E V, Yurakov Yu A, Rudneva I G and Domashevskaya E P 2002 Electronic structure of rhenium disilicides *J. Phys.: Condens. Matter* **14** 6833–9

[14] Jiang H, Petersson C S and Nicolet M-A 1986 Thermal oxidation of transition metal silicides *Thin Solid Films* **140** 115–30

For β-$FeSi_2$ oxidation see Rebien M, Henrion W, Angermann H and Röseler A 2000 Ellipsometric comparison of the native oxides of silicon and semiconducting iron disilicide (β-$FeSi_2$) *Surf. Sci.* **462** 143–50

[15] Brixner D 1985 *Handbook of Optical Constants of Solids* ed E D Palik (New York: Academic) p 759

[16] Kresse G and Hafner J 1994 *Ab initio* molecular-dynamics simulation of the liquid-metal–amorphous–semiconductor transition in germanium *Phys. Rev.* B **49** 14251–69

Kresse G and Furthmüller J 1996 Efficiency of *ab-initio* total energy calculations for metals and semiconductors using a plane-wave basis set *J. Comput. Mater. Sci.* **6** 15–50

Kresse G and Furthmüller J 1996 Efficient iterative schemes for *ab initio* total-energy calculations using a plane-wave basis set *Phys. Rev.* B **54** 11169–86

[17] Ceperly D M and Alder B J 1980 Ground state of the electron gas by a stochastic method *Phys. Rev. Lett.* **45** 566–9

Perdew J and Zunger A 1981 Self-interaction correction to density-functional approximations for many-electron systems *Phys. Rev.* B **23** 5048–79

[18] Blaha P, Schwarz K, Madsen G K H, Kvasnicka D and Luitz J 2001 *WIEN2k, An Augmented Plane Wave + Local Orbitals Program for Calculating Crystal Properties* ed Karlheinz Schwarz (Vienna: Techn. Universität Wien) ISBN 3-9501031-1-2

[19] Migas D B, Miglio L, Shaposhnikov V L and Borisenko V E 2002 Structural, electronic and optical properties of isostructural Ru_2Si_3, Ru_2Ge_3, Os_2Si_3 and Os_2Ge_3 *Phys. Status Solidi* b **231** 171–80

[20] Moroni E G, Wolf W, Hafner J and Podloucky R 1999 Cohesive, structural, and electronic properties of Fe–Si compounds *Phys. Rev.* B **59** 12860–71

[21] Misra A, Chu A and Mitchell T E 1998 Elastic properties of the intermetallic compound $ReSi_2$ *Scr. Mater.* **38** 917–21

[22] Mattheiss L F 1991 Structural effects on the calculated semiconductor gap of $CrSi_2$ *Phys. Rev.* B **43** 1863–6

[23] Filonov A B, Tralle I E, Dorozhkin N N, Migas D B, Shaposhnikov V L, Petrov G V, Anishchik V M and Borisenko V E 1994 Semiconducting properties of hexagonal chromium, molybdenum, tungsten disilicides *Phys. Status Solidi* b **186** 209–15

[24] Filonov A B, Migas D B, Shaposhnikov V L, Dorozhkin N N, Petrov G V, Borisenko V E, Henrion W and Lange H 1996 Electronic and related properties of crystalline semiconducting iron disilicide *J. Appl. Phys.* **79** 7708–12

[25] Migas D B, Miglio L, Henrion W, Rebien M, Marabelli F, Cook B A, Shaposhnikov V L and Borisenko V E 2001 Electronic and optical properties of isostructural β-$FeSi_2$ and $OsSi_2$ *Phys. Rev.* B **64** 075208

[26] Migas D B and Miglio L 2000 Band-gap modifications of β-$FeSi_2$ with lattice distortions corresponding to the epitaxial relationships on Si(111) *Phys. Rev.* B **62** 11063–70

[27] Hofman D, Kleint C, Thomas J and Wetzig K 2000 Investigation of thermoelectric silicide thin films by means of analytical transmission electron microscopy *Ultramicroscopy* **81** 271–7